Iranian Journal of Basic Medical Sciences

ijbms.mums.ac.ir

IJBMS

S100A9 aggravates bleomycin-induced dermal fibrosis in mice via activation of ERK1/2 MAPK and NF-κB pathways

Xue Xu [1], Zhiyong Chen [1], Xiaoxia Zhu [2], Dandan Wang [1], Jun Liang [1], Cheng Zhao [1], Xuebing Feng [1], Jiucun Wang [3], Hejian Zou [2], Lingyun Sun [1*]

[1] Department of Rheumatology and Immunology, Nanjing Drum Tower Hospital, the Affiliated Hospital of Nanjing University Medical School, Nanjing 210008, Jiangsu, China
[2] Division of Rheumatology, Huashan Hospital, Fudan University, Shanghai 200040, China
[3] State Key Laboratory of Genetic Engineering and Ministry of Education Key Laboratory of Contemporary Anthropology, School of Life Sciences, Fudan University, Shanghai 200433, China

ARTICLEINFO

Article type:
Original article

Article history:
Received: Nov 6, 2016
Accepted: Sep 28, 2017

Keywords:
Bleomycin
ERK1/2 MAPK
NF-κB
RAGE
S100A9
Scleroderma

ABSTRACT

Objective(s):This study aims to investigate the pathogenicity and possible mechanisms of S100A9 function in mice models of scleroderma.

Materials and Methods: The content of S100A9 in the skin tissues of mice with scleroderma was determined. Different concentrations of bleomycin (BLM) and S100A9 were subcutaneously injected into the backs of mice simultaneously, and then pathological changes in the skin of these mice were monitored. Specifically, the levels of inflammatory cytokines and alpha smooth muscle actin (α-SMA), the activation of extracellular regulated kinase 1/2 (ERK1/2), mitogen-activated protein kinase (MAPK) and nuclear factor-kappa B (NF-κB) pathways, and the expression of the receptor for advanced glycation end-product (RAGE) in the skin were determined.

Results: The content of S100A9 in the skin tissues of mice with scleroderma was determined. Different concentrations of BLM and S100A9 were subcutaneously injected into the backs of mice simultaneously, and then pathological changes in the skin of these mice were monitored. Specifically, the levels of inflammatory cytokines and alpha smooth muscle actin (α-SMA), the activation of extracellular regulated kinase 1/2 (ERK1/2) mitogen-activated protein kinase (MAPK) and nuclear factor-kappa B (NF-κB) pathways, and the expression of the receptor for advanced glycation end-product (RAGE) in the skin were determined.

Conclusion: S100A9 aggravates dermal fibrosis in BLM-induced scleroderma (BIS) mice, and its mechanisms might be mediated by RAGE, ERK1/2, and NF-κB pathway.

► *Please cite this article as:*
Xu X, Chen Zh, Zhu X, Wang D, Liang J, Zhao Ch, Feng X, Wang J, Zou H, Sun L. S100A9 aggravates bleomycin-induced dermal fibrosis in mice via activation of ERK1/2 MAPK and NF-κB pathways. Iran J Basic Med Sci 2018; 21:194-201. doi: 10.22038/IJBMS.2018.19987.5255

Introduction

Scleroderma is a connective tissue disease caused by the excessive synthesis and deposition of extra -cellular matrix (ECM) in skin and internal organs, which subsequently cause the fibrotic hardening and dysfunction of those tissues and organs (1). This disease currently has no specific drug or treatment method, and the main causes of death include pulmonary hypertension, pulmonary interstitial fibrosis, secondary-pulmonary infection, or renal failure (2). The pathogenesis of scleroderma remains unclear, and now it is considered related to immune abnormalities, blood vascular abnormalities, or connective tissue dysmetabolism. Therefore, further study of its mechanisms and actively searching for new targets for its treatment would have therapeutic significance.

The S100 protein family is a group of calcium-binding proteins with similar structures and functions. S100A9 has a molecular weight that is relatively lower than that of the other family members, and is also known by several different names such as myeloid-related protein 14 (MRP14) and calgranulin B (3). S100A9 is mainly derived from secretions from myeloid-derived cells such as monocytes, neutrophils, and macrophages during early differentiation (4), and its function is related to the body's innate immune system. Several studies have found that S100A9 is a potent neutrophil chemoattractant (5), and can promote all types of cells to secret inflammatory cytokines such as interleukin (IL)-6, IL-8, or tumor necrosis factor (TNF)-α. Thus, it appears that S100A9 plays an important role in inflammatory processes, and this is supported by the fact that it is associated with a variety of inflammatory and autoimmune diseases (6).

It is currently known that the course of scleroderma

*Corresponding author: Lingyun Sun. Department of Rheumatology and Immunology, Nanjing Drum Tower Hospital, the Affiliated Hospital of Nanjing University Medical School, No. 321 Zhongshan Road, Nanjing 210008, Jiangsu, China. Tel: +86-25-83106666-61421; Fax:+862568182428; Email: lingysun@sina.com

could be divided into the early in flammation and late fibrosis stages. Most studies suggest that the early inflammatory reactions were the main factors that further promoted the activation of fibroblasts and induced tissue fibrosis (7). Few studies discuss the possibility of the proinflammatory cytokine S100A9 playing a role in the pathogenesis of scleroderma. However, existing data indicate that the levels of S100A9 in the peripheral blood cells, saliva, and alveolar lavage of patients with systemic sclerosis are higher than the levels in healthy individuals (8-10). Moreover, one study performed a proteomic analysis of plasma S100A8/S100A9 levels and found that they were significantly increased in patients with systemic sclerosis (11). In our previous studies, we had confirmed that the levels of S100A9 were significantly increased in the peripheral blood of patients with systemic sclerosis, and that the inflammatory cells and fibroblasts that expressed S100A9 in the skin lesions of patients with scleroderma were also significantly increased (12). This suggests that S100A9 may play a role in the processes of skin inflammation and fibrosis.

In this study, we used an animal model to study the impact of S100A9 on skin fibrosis. Bleomycin (BLM), which is an essential glycopeptide antibiotic produced by *Streptomyces* and used in anti-tumor therapies, is the most widely used medicine to induce scleroderma. The side effects of BLM use include pulmonary fibrosis, dermal fibrosis, keratosis, Raynaud's phenomenon, pigmentation, and alopecia. The mechanism by which these conditions arise involves the activation of inflammatory cells and the secretion of inflammatory factors and chemokines. Moreover, BLM increases the production of free radicals, which induce endothelial cells and fibro - blasts to increase the synthesis of the ECM and induce fibrosis (13).

To clarify the role of S100A9 in scleroderma, we analyzed S100A9 expression in the mice models and injected mice simultaneously with S100A9 and BLM so as to observe whether S100A9 could promote the skin of BLM-induced scleroderma mice to harden, and to discuss the possible mechanisms. This is the first step towards understanding whether S100A9 may be a trigger molecule involved in the progression of scleroderma.

Materials and Methods

Preparation of animal model

All C57BL/6 mice (SPF grade, female, and 6-weeks old) were purchased from the Experimental Animal Center, Shanghai Institutes for Biological Sciences, CAS. These mice were randomly divided into three groups (n=6), and the back of each mice was subcutaneously injected different drugs: a control group (100 μl of 0.9% saline solution), a low-dose BLM group (100 μl of 0.2 mg/ml BLM) and a high-dose BLM group (100 μl of 0.3 mg/ml BLM). Another set of 6-week-old C57BL/6 mice were randomly divided into five groups (n=6): a control group (injected with 100 μl of 0.9% saline solution at 8 am), a S100A9 group (injected with 100 μl of 5 μg/ml S100A9 at 8 am), a low-dose BLM group (injected with 100 μl of 0.2 mg/ml BLM at 8 am), a low-dose BLM + S100A9 group (injected with 100 μl of 0.2 mg/mL BLM at 8 am, and injected with 100 μl of S100A9 5 μg/ml at 4 pm), a high-dose BLM group (injected with 100 μl of 0.3 mg/ml BLM at 8 am, as the positive control). Three weeks after the medication, all mice were killed by cervical dislocation, and the diseased skin at the injection site was cut for further study. This study was carried out in strict accordance with the recommendations in the Guide for the Care and Use of Laboratory Animals of the National Institutes of Health. The animal use protocol has been reviewed and approved by the Institutional Animal Care and Use Committee (IACUC) of Nanjing University.

Staining of skin tissues

The diseased skin was immediately sampled after the sterile euthanization of the mice and paraffin sections were prepared. The sections were subjected to hematoxylin-eosin (HE) staining and Masson specific staining; the differences between the experimental groups and the control group were then observed under a microscope.

Real time-polymerase chain reaction (RT-PCR)

The RNA from the mice skin samples was extracted using Trizol and reverse transcribed into cDNA using reverse transcriptase (TaKaRa, Shiga, Japan). The ABI Prism 7500 PCR amplification instru - ment (Applied Biosystems, Foster City, CA, USA) was used for all PCR amplification with GAPDH being set as the internal reference. The relative expression of the target gene mRNA was then calculated (Table 1).

Table 1 Primer of gene in fluorescent quantitative real time-polymerase chain reaction

Protein content	Gene primer	bp
S100A9	CAAATGGTGGAAGCACAGTT AGCATCATACACTCCTCAAAGC	163
IL-6	TGTGAAGGTCAACCTCAAAGTC AGGGATATCTATCAGGGTCTTCATT	149
IL-1β	AAGGAGAACCAAGCAACGACAAAA TGGGGAACTCTGCAGACTCAAACT	216
IL-8	CTGACGGCACAGAGCTATTGA GAGATGTTGCTCAGCTCCTCA	207
TNF-α	GCCAGCCCACAGTTCTACAGC GAGATGTTGCTCAGCTCCTCA	193
RAGE	GTGCTATGACGATGGGAAGA CCAGGTCTACGGCAGTTGT	148
α-SMA	TCACCATGCCCTCTACAAGA TCACCATCGCAAGGAACTC	182
GAPDH	AACTCCCACTCTTCCACCTTCG TCCACCACCCTGTTGCTGTAG	243

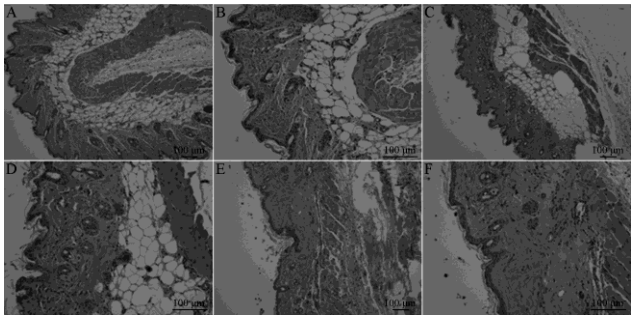

Figure 1. Hematoxylin-eosin staining results of mice's skin tissues. 18 C57BL/6 mice were randomly divided into three groups, and then subcutaneously injected saline (A, B), low-dose BLM (C, D), and high dose BLM (E, F) for 3 consecutive weeks, respectively. Three weeks later, these mice were killed, and the skin tissues at the injection site were sampled for HE staining to observe the pathological changes

Western blot

Skin samples were cut into pieces and added to 1 ml RIPA buffer (PMSF was added according the ratio). An electromotion stirrer at 1000 RPM was used to homogenize the tissues while on crushed ice to avoid protein degradation. Homogenates were then transferred into a sterile Eppendorf tube and shocked for 10 sec, after which they were left to stand for 60 min on ice with vortexing for 10 sec every 15 min. Samples were then centrifuged for 43800 g for 15 min at 4°C. The supernatant was then transferred into an Eppendorf tube and the protein concentration was determined by ultraviolet spectrophotometry.

Samples were then prepared for sodium dodecyl sulfate-polyacrylamide gel electrophoresis (SDS-PAGE). Specifically, 40 µl of the supernatant was added to 10 µl SDS and boiled for 5 min. These samples were then frozen at -80°C until use. Thirty micrograms of protein from each sample was then loaded on a 10% SDS-gel and the gel was run at 4°C. This gel was then transferred onto a PVDF membrane. The PVDF membranes were then cut according to the targeted band regions and the marker positioning, and blocked for 2 hr with 5% skimmed milk. The membranes were then incubated overnight with different primary antibodies at 4°C: rabbit polyclonal anti-human alpha smooth muscle actin (α-SMA) (Epitomics, Burlingame, CA, USA), rabbit polyclonal anti-human receptor for advanced glycation end-product (RAGE; Abgent, San Diego, CA, USA), phospho-extracellular regulated kinase mitogen activated protein kinase (p-ERK MAPK; Signaling Technology, Danvers, MA, USA), and nuclear factor-kappa B (NF-κB) family antibody (Santa Cruz, CA, USA). The horseradish peroxidase-labeled secondary antibody (1:1000) (Jackson-Immuno, West Grove, PA, USA) was then added and shaken at room temperature for 2 hr. The membranes were then washed and developed using coloration liquids, and a gel image processing system (LAS-3000 plus; Fuji Photo film, Tokyo, Japan) was used to analyze the target proteins imaged after different exposure times.

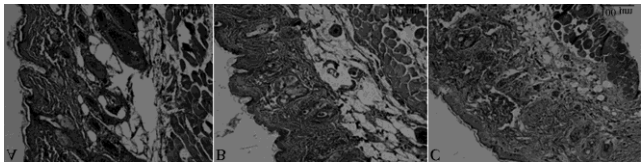

Figure 2. Masson staining results of mice's skin tissues
18 C57BL/6 mice were randomly divided into three groups, and then subcutaneously injected saline (A), low-dose BLM (B), and high dose BLM (C) for 3 consecutive weeks, respectively. Three weeks later, these mice were killed, and the skin tissues at the injection site were sampled for Masson staining

Data processing and statistical analysis

SPSS12.0 software package was used for the statistical analysis, and the data were expressed as mean±standard deviation ($\bar{x}$ ±SD). The inter-group comparison used the Student's *t*-test or one-way ANOVA, with $P<0.05$ considered statistically significant.

Results

Identification of BIS mouse model

The results of HE staining showed that compared with that in the control group (Figure 1A, B), the skin lesions of the mice in group H were significantly thickened, there was an increase in the bundles of collagen fibers, and the amount of fat tissue was significantly reduced (Figure 1 E, F). The dermis of the mice in group L exhibited a small amount of coarse collagen fibers, but no sebaceous gland or sweat gland shrank, and the subcutaneous adipose tissue showed no significant reduction (Figure 1C, D). The Masson staining showed that compared with that in the control group (Figure 2A), the mandarin blue-stained collagen fibers in the dermis of the mice in group H were proliferated and accumulated, and the subcutaneous adipose tissue was also replaced by collagen fibers (Figure 2C). The same staining in group L was lighter, and there was less proliferation with no significant accumulation of collagen being found (Figure 2B). These results suggested that high-dose BLM could significantly induce fibrosis and sclerosis in the back skin tissues of C57BL/6 mice, but low-dose BLM could not induce such changes.

S100A9 was increased in the skin of BIS mice

High-dose BLM could cause scleroderma-like changes to the dorsal skin of C57BL/6 mice. The pathological changes in group L were not obvious, so we used high-dose BLM to treat the mice. The PCR results showed that compared with that in the control group, the S100A9 mRNA expression in one-week BIS-treated mice was significantly increased, which was also gradually increased with the BLM induction extension (Figure 3A). The results of the Western blot analysis further found that the expression of S100A9

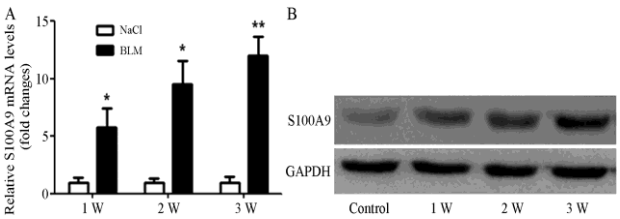

Figure 3. Changes of S100A9 expression in the skin tissues of BIS mice
The C57BL/6 mice were then continuously injected BLM, but the control mice were injected saline. The mice were killed in the 1st, 2nd, and 3rd week, respectively, and the S100A9 expression in the skin was detected using real-time PCR (A), and the S100A9 content in the skin was detected using Western blot (B). Compared with the control group, **P*<0.05, *P*<0.01

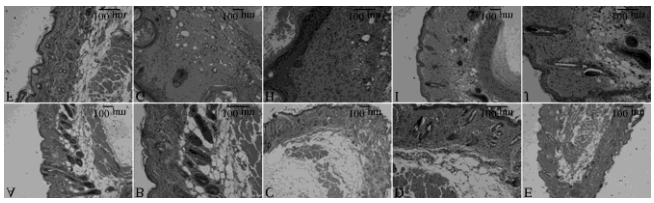

Figure 4. Hematoxylin-eosin staining results of mice's skin tissues
The C57BL/6 mice were randomly divided into five groups (n=six), and subcutaneously administrated saline (A, B), S100A9 (C, D), low-dose BLM (E, F), low-dose BLM +S100A9 (G, H), and high-dose BLM (I, J). The skin tissues at the injection site were sampled three weeks later for the HE staining. Followed by the pathological observation under one microscope

protein began to increase one week after BLM stimulation, and reached a peak in the 3rd week (Figure 3B). These results suggest that during the inflammation and fibrosis processes in the skin tissues of BIS-treated mice, the S100A9 content in the skin increased significantly.

Impacts of S100A9 on BIS

To investigate whether S100A9 had a pathogenic role, we observed whether S100A9 could promote skin hardening in group L. In this study, low-dose BLM and S100A9 were subcutaneously injected simultaneously, and the skin in group H was used as the positive control.

The results of HE staining suggested that compared with that in the control group (Figure 4A, B), the dermis in group L showed no significant deposition of collagen fibers (Figure 4E, F). Conversely, the collagen bundles in the dermis of group BLM+S100A9 were coarse, homogenized, and abundant, exhibiting significant collagen deposition. Additionally, a large number of inflammatory cells infiltrated the collagen bundles, and the hair follicles' sebaceous glands and sweat glands had basically disappeared along with the adipose tissue (Figure 4G, H). Compared with group BLM+S100A9, the dermis in group H still had a small amount of sebaceous glands and sweat glands, and some subcutaneous adipose tissue still remained (Figure 4I, J).

Table 2. Thickness of diseased skin (epidermis+ dermis) in different groups

Group	n	Skin thickness ($\bar{X}$ ±SD) (μm)
Control	6	159.92±27.03
S100A9	6	213.75±30.21*
L	6	204.75±34.72
BLM+S100A9	6	764.39±123.47*#&
H	6	290.58±52.68*#

The color pathological image analysis system was used to determine the skin thickness, and each mouse was randomly sampled five skin biopsies for measuring the skin thickness (epidermis+dermis); the mean and standard difference was also calculated. * compared with the control Group, *P*<0.05, # compared with group L, *P*<0.01, & compared with group H, *P*<0.01

The microscopic image analysis system was used to detect the skin thickness of each group, and the results showed that the skin thickness comparison between group L and the control group had no statistical significance. However, after S100A9 was injected, the skin thickness significantly increased (Table 2). In addition, the skin thickness in group BLM+S100A9 was three times that in group H (*P*<0.01).

The results of Masson staining showed that compared with that in the control group (Figure 5A), the collagen fibers in group L were slightly proliferated (Figure 5C). The collagen fibers in the dermal layer of group BLM+S100A9 were deeply blue-stained, exhibiting significant proliferation and accumulation, and the subcutaneous adipose tissues were almost invisible (Figure 5E). Alternatively, the collagen fibers in the dermal layer of group H exhibited obvious proliferation, but normal glands and adipose tissues could be seen among these proliferated collagen fibers (Figure 5D). Therefore, the accumulation of collagen fibers in the dermal layer of group BLM+S100A9 was more significant than in group H.

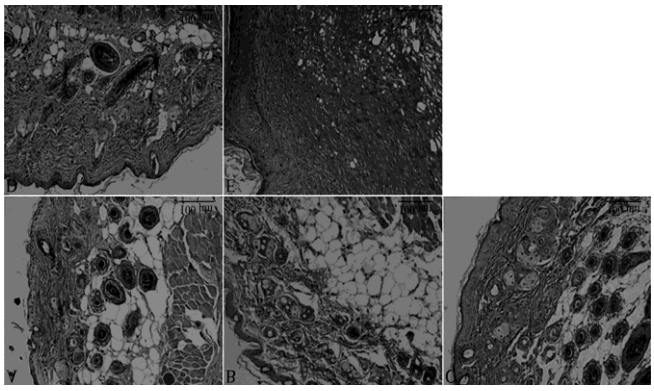

Figure 5. Masson staining results of mice's skin tissues
The C57BL/6 mice were randomly divided into five groups (n=six), and subcutaneously given saline (A), S100A9 (B), low-dose BLM (C), high-dose BLM (D), and low-dose BLM +S100A9 (E), respectively, for three consecutive weeks. The mice were then killed and sampled the skin for the Masson specific staining

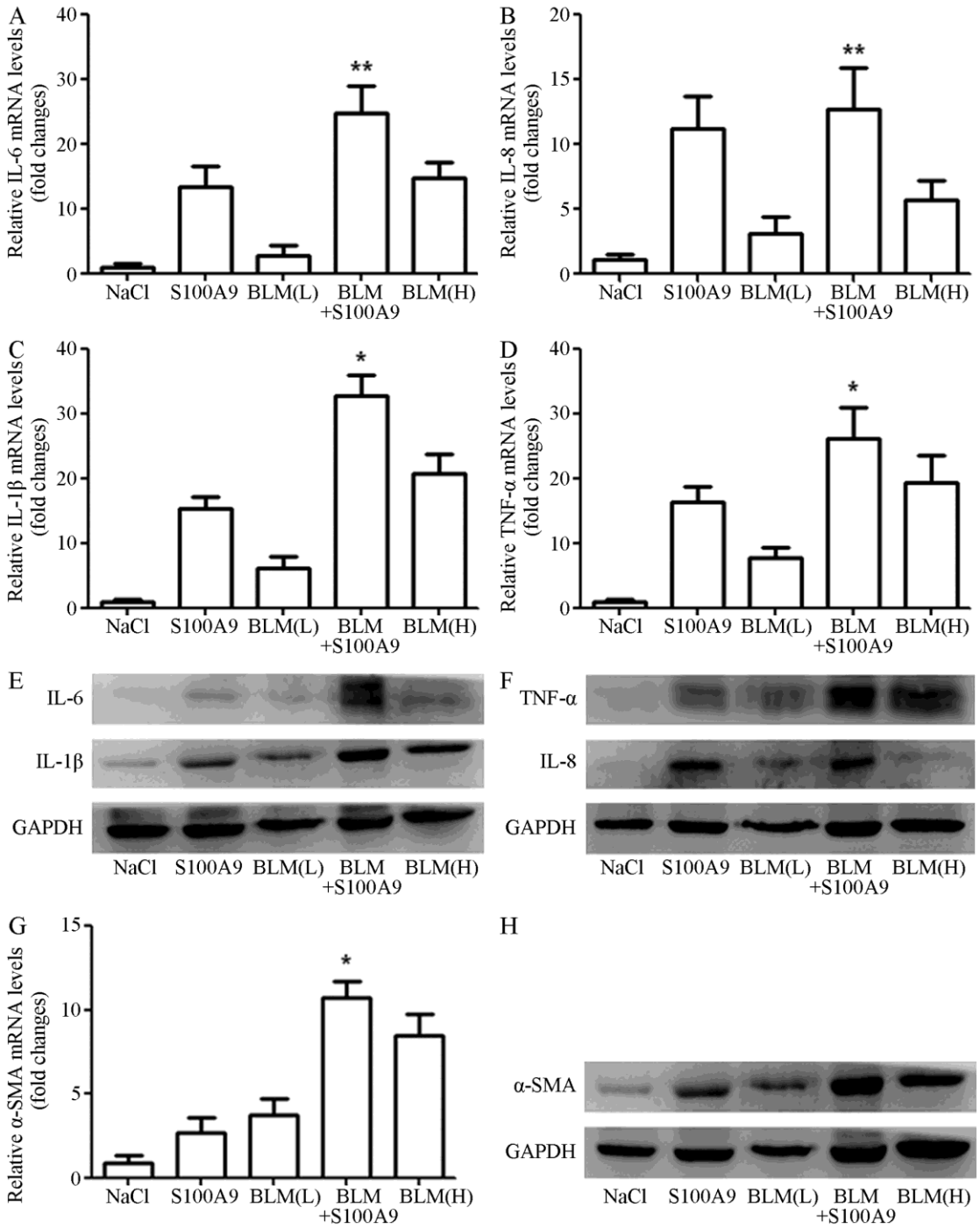

Figure 6. Expression of inflammatory cytokines and α-SMA in the skin tissues of different groups
The C57BL/6 mice were randomly divided into five groups (n=six), and subcutaneously injected saline, S100A9, low-dose BLM, low-dose BLM+S100A9, and high-dose BLM, respectively, for three consecutive weeks. The mice were then killed and sampled the skin lesions for detecting the expressions of IL-6 (A), IL-1β (B), IL-8 (C), TNF-α (D), and α-SMA (F) by real-time PCR, and the contents of IL-6, IL-1β, IL-8, TNF-α (E), and α-SMA (G) by Western blot. Compared with group H, **P*<0.05, ***P*<0.01

We found that the mRNA expression levels of inflammatory cytokines IL-6, IL-1β, IL-8, and TNF-α in the skin of group BLM+S100A9 increased significantly, and were all higher than the levels in group H (Figure 6A–D). In addition, Western blots revealed that the protein levels of the above inflammatory cytokines in the skin tissues of group BLM+S100A9 were also signi - ficantly higher than in group L and H (Figure 6E). Moreover, the protein and mRNA expression levels for α-SMA were higher in the BLM+S100A9 group as compared to those in group H (Figure 6F, G).

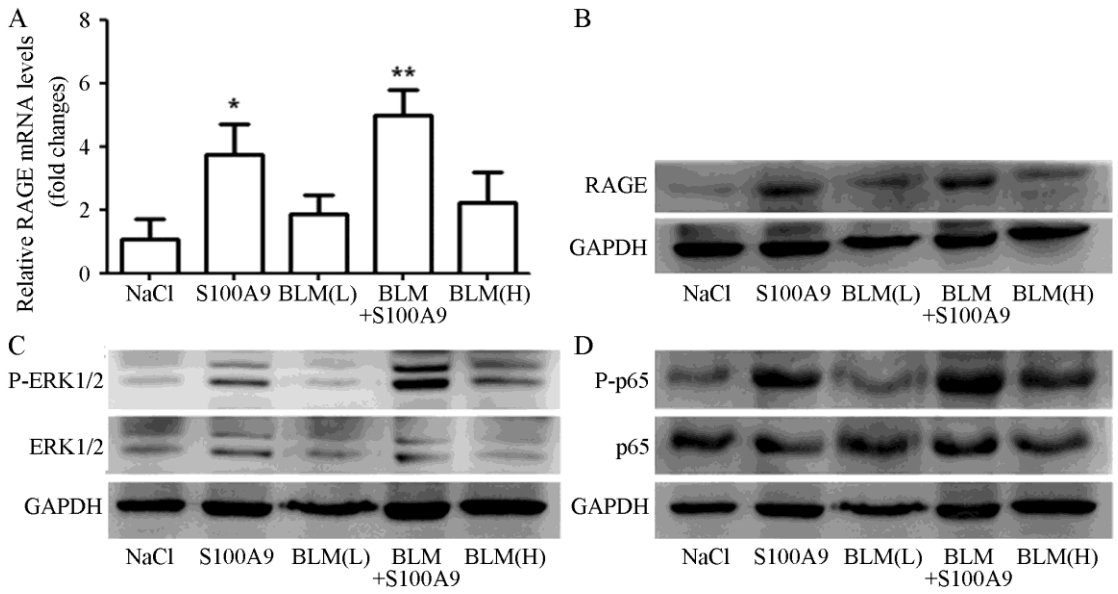

Figure 7. Impacts of S100A9 on the ERK1/2 MAPK and NF-κB pathways and the expression level of RAGE in mouse skin tissues. The C57BL/6 mice were randomly divided into five groups (n=six), and subcutaneously injected saline, S100A9, low-dose BLM, low-dose BLM+S100A9, and high-dose BLM, respectively, for three consecutive weeks. The mice were then killed and sampled the skin lesions for detecting the expression level of RAGE by fluorescence quantitative PCR and Western blot (A, B), and the activation of ERK1/2 MAPK and NF-κB pathways (C) by Western blot. Compared with the control group, *P<0.05, **P<0.01

S100A9 could promote the activation of extracellular regulated kinase 1/2 (ERK1/2) and NF-κB signaling pathways in mouse skin tissues

As shown in Figure 7A and B, the RAGE expression in either group L or H showed no significant difference when compared to the control group. The subcutaneous injection of S100A9 enhanced RAGE expression, and the RAGE content in group BLM+S100A9 also increased significantly, suggesting that S100A9 could promote the synthesis of RAGE in mouse skin tissues.

We failed to detect any significant phosphorylation of ERK1/2 MAPK and NF-κB in group L, although those proteins in group H were slightly phosphorylated. Conversely, ERK1/2 MAPK and NF-κB proteins in group BLM+S100A9 were significantly phosphorylated (Figure 7C).

Discussion

The current study showed that the S100A9 level in the skin of sclerodermatous mice was significantly increased as compared to the control group. A low-dose of BLM could not induce mouse skin to form typical scleroderma-like lesions, but the simultaneous administration of S100A9 with low-dose BLM was able to promote local skin hardening in group L. Meanwhile, the skin thickness was significantly increased, and the expressions of intra-skin inflammatory cytokines, collagens, and α-SMA were increased. This indicates that the pro-fibrotic effects of the combination of these two substances were much stronger than a high-dose of BLM. Furthermore, the simultaneous administration of S100A9 with low-dose BLM enhanced the phosphorylation of ERK1/2 MAPK and NF-κB in mouse skin tissues, and promoted the expression of RAGE. Therefore, the above results suggest that S100A9 plays an important role in the pathogenesis of dermal fibrosis in scleroderma, which might possibly be realized through the participation of RAGE, and the ERK1/2 MAPK and NF-κB signaling pathways.

A large amount of data has confirmed that S100A9 expression is closely related to many inflammatory and autoimmune diseases. Moreover, the expression of S100A9 has been found to be increased in the synovial fluid, plasma, and feces of patients with rheumatoid arthritis, systemic lupus erythematosus, vasculitis, and inflammatory bowel diseases, suggesting that S100A9 could be a biomarker for such diseases (14). Currently, there are few reports about scleroderma and S100A9, and our previous study found that the skin of patients with scleroderma showed increased expression of S100A9 (11). We further confirmed using the sclerodermatous mouse model that after 1-, 2-, and 3-weeks of BLM induction, the levels of S100A9 in the skin increased gradually, indicating that during the BIS process, S100A9 was upregulated in the skin lesions from the inflammatory phase to the fibrosis stage. Studies had shown that in the pulmonary lavage fluid of BIS mice, the S100A8 concentration was increased, and the neutrophil count with positive S100A8 in lung tissues increased significantly (15). This suggests that during BIS, the high concentration of S100A8 could recruit inflammatory cells to infiltrate the lungs and participate in the disease progression. S100A9 and S100A8 belong to the S100 protein family, and their structures are very similar (16). Indeed, they both are

known to play an important role in neutrophil functioning. With respect to S100A9, its content in diseased human skin and in the BIS mouse model were both significantly upregulated compared to that in healthy individuals, suggesting that S100A9 may play a similar proinflammatory role as S100A8 in the progression of skin lesions.

To better understand whether S100A9 was involved in the pathogenesis of scleroderma, S100A9 and low-dose BLM were subcutaneously injected in mice simultaneously. While a low-dose of BLM alone could not induce fibrosis of the mouse skin, skin lesions did appear in the BLM+S100A9 group of mice and both the dermis and epidermis was markedly thickened, which is consistent with the literature (17). The results of HE and Masson staining showed that the collagen fibers in the dermal layer of the BLM+S100A9 group increased, the fat tissues totally disappeared, and there was a large infiltration of inflammatory cells. Interestingly, a small amount of sub endothelial fatty tissues in the dermal layer in group H remained. These results suggested that the skin fibrosis in the BLM+S100A9 group was much more severe than that in group H, indicating that low-dose BLM could not induce fibrosis, but S100A9 could assist low-dose BLM to induce skin sclerosis. These effects were even greater than that found in the high-dose BLM treatment. Recent studies have found that the skin of patients with systemic sclerosis could secrete large amounts of S100A9, which could promote the proliferation and migration of dermal fibroblasts, and induce the fibroblasts to express the pro-fibrotic factor CCN2 (18). This would suggest that S100A9 might participate in the pathogenesis of scleroderma through inducing pro-fibrotic factors.

We also found that the expression of IL-6, IL-8, IL-1β, and TNF-α in the skin tissues of the BLM+S100A9 group increased significantly, higher than those in groups L and H. This is consistent with the strong proinflammatory properties of S100A9. Furthermore, S100A9 appeared to elevate the expression of α-SMA in the BLM+S100A9 group, significantly higher than that in group H (Figure 6F–G). *In vitro* studies have found that S100A9 could induce human lung fibroblasts (HLF) to secrete IL-6, IL-8, IL-1β, or other inflammatory factors, and to promote HLF to synthesize α-SMA (19). Importantly, the above inflammatory cytokines have been confirmed to participate in the pathogenesis of scleroderma (20–22). Moreover, α-SMA is the mark antibody of myofibroblasts, and S100A9 could induce the fibroblasts to converse toward myofibroblasts, which are the main cells to synthesize matrix collagens. Therefore, we hypothesized that S100A9 possessed pro-inflammation and pro-fibrosis characteristics, and might play an important role in the pathogenesis of scleroderma.

Existing data has shown that RAGE is a member of the cell surface immunoglobulin superfamily and that it is widely distributed and expressed on the cell surface of mononuclear macrophages, epithelial cells, vascular endothelial cells, and tumor cells (23). RAGE participates in such physiological processes as cell proliferation, differentiation, and inflammation (24). It has been demonstrated that multiple members of the S100 protein family are endogenous ligands of RAGE (25). We found that S100A9 significantly increase the RAGE content in the skin tissues of the BLM+S100A9 group, suggesting that S100A9 could induce the mouse skin to synthesize RAGE. Interestingly, RAGE was found to participate in the pathogenesis of interstitial lung disease, regulate the degradation of the ECM, induce epithelial cells to transform toward interstitial cells, and promote fibrotic lung remodeling caused by the migration and adhesion of neutrophils toward fibronectin (26, 27). This suggests that RAGE could be a new factor in inducing fibrosis. Another study also found that a S100 protein promoted cardiac fibroblasts to upregulate the expression of fibroblast growth factor (FGF) 23, and aggravated left ventricular hypertrophy and aortic calcification in mice with chronic kidney disease in a RAGE-dependent manner (28). We speculated that S100A9 might interact with fibroblasts via RAGE, thus activating the cells and playing a pro-fibrosis role. Our previous experiments revealed that S100A9 could activate cells by stimulating the phosphorylation of ERK1/2 MAPK and NF-κB pathways in HLF cells (12). In our animal experiments, we found that S100A9 administered alone could cause the phosphorylation of members of ERK1/2 MAPK and NF-κB pathways in mouse skin tissues, but these phosphorylation events were enhanced when BLM and S100A9 were administered simultaneously. This suggests that the activation of ERK1/2 MAPK and NF-κB pathways played an important role in the process of S100A9-induced mouse skin fibrosis.

Conclusion

In summary, our study revealed that S100A9 exacerbated skin fibrosis in a mouse model of scleroderma, and enhanced the expression of RAGE and the activation of ERK1/2 MAPK and NF-κB signaling pathways in the skin tissues. These results suggest that this factor played an important role in the pathogenesis of scleroderma. Since S100A9 appears to be involved in the pathogenesis of this disease, it may be a new target for the treatment of scleroderma. Further studies will be necessary to determine exactly how S100A9 could activate human skin fibroblasts and cause disease.

Acknowledgment

This work was supported by National Natural Science Foundation of China (No.81501409).

Conflict of interest

All of the authors declare that they have no conflicts of interest regarding this paper.

References

1. Varga J, Abraham D. Systemic sclerosis: a prototypic multisystem fibrotic disorder. J Clinical Invest 2007;117:557-567.
2. Yanaba K. Strategy for treatment of fibrosis in systemic sclerosis: Present and future. J Dermatol 2016;43:46-55.
3. Foell D, Wittkowski H, Vogl T, Roth J. S100 proteins expressed in phagocytes: a novel group of damage-associated molecularpattern molecules. J LeukocBiol 2007;81:28-37.
4. Ryckman C, Gilbert C, de Médicis R, Lussier A, Vandal K, Tessier PA. Monosodium urate monohydrate crystals induce the release of the proinflammatory protein S100A8/A9 from neutrophils. J LeukocBiol 2004;76:433-440.
5. Simard JC, Girard D, Tessier PA. Induction of neutrophil degranulation by S100A9 via a MAPK-dependent mechanism. J LeukocBiol 2010;87:905-914.
6. Schnekenburger J, Schick V, Krüger B, Manitz MP, Sorg C, Nacken W, *et al*. The calcium binding protein Sl00A9 is essential for pancreatic leukocyte infiltration and induces disruption of cell-cell contacts. J Cell Physiol 2008;216:558-567.
7. Kurzinski K, Torok KS. Cytokine profiles in localized scleroderma and relationship to clinical features. Cytokine 2011;55:157-164.
8. Tan FK, Zhou X, Mayes MD, Gourh P, Guo X, Marcum C, *et al*. Signatures of differentially regulated interferon gene expression and vasculotrophism in the peripheral blood cells of systemic sclerosis patients. Rheumatology (Oxford) 2006;45:694-702.
9. Giusti L, Bazzichi L, Baldini C, Ciregia F, Mascia G, Giannaccini G, *et al*. Specific proteins identified in whole saliva from patients with diffuse systemic sclerosis. J Rheumatol 2007;34:2063-2069.
10. Fietta A, Bardoni A, Salvini R, Passadore I, Morosini M, Cavagna L, *et al*. Analysis of bronchoalveolar lavage fluid proteome from systemic sclerosis patients with or without functional, clinical and radiological signs of lung fibrosis. Arthritis Res Ther 2006;8:R160.
11. van Bon L, Cossu M, Loof A, Gohar F, Wittkowski H, Vonk M, *et al*. Proteomic analysis of plasma identifies the Toll-like receptor agonists S100A8/A9 as a novel possible marker for systemic sclerosis phenotype. Ann Rheum Dis 2014;73:1585-1589.
12. Xu X, Wu WY, Tu WZ, Chu HY, Zhu XX, Liang MR, *et al*. Increased expression of S100A8 and S100A9 in patients with diffuse cutaneous systemic sclerosis. A correlation with organ involvement and immunological abnormalities. Clin Rheumatol 2013;32:1501-1510.
13. Yamamoto T, Nishioka K. Cellular and molecular mechanisms of bleomycin-induced murine scleroderma: current update and future perspective. ExpDermatol 2005;14:81-95.
14. Foell D, Roth J. Proinflammatory S100 proteins in arthritis and autoimmune disease. Arthritis Rheum 2004;50:3762-3771.
15. Kumar RK, Harrison CA, Cornish CJ, Kocher M, Geczy CL. Immunodetection of the murine chemotactic protein CP-10 in bleomycin-induced pulmonary injury. Pathology 1998;30:51-56.
16. Kerkhoff C, Klempt M, Sorg C. Novel insights into structure and function of MRP8 (S100A8) and MRP14 (S100A9). BiochimBiophysActa 1998;1448:200-211.
17. Yamamoto T, Kuroda M, Nishioka K. Animal model of sclerotic skin. III: Histopathological comparison of bleomycin-induced scleroderma in various mice strains. Arch Dermatol Res 2000;292:535-541.
18. Nikitorowicz-Buniak J, Shiwen X, Denton CP, Abraham D, Stratton R. Abnormally differentiating keratinocytes in the epidermis of systemic sclerosis patients show enhancedsecretion of CCN2 and S100A9. J Invest Dermatol 2014;134:2693-2702.
19. Xu X, Chen H, Zhu X, Ma Y, Liu Q, Xue Y, *et al*. S100A9 promotes human lung fibroblast cells activation through receptor for advanced glycation end-product-mediated extracellular-regulated kinase 1/2, mitogen-activated protein-kinase and nuclear factor-κB-dependent pathways. ClinExpImmunol 2013;173:523-535.
20. Fullard N, O'Reilly S. Role of innate immune system in systemic sclerosis. SeminImmunopathol 2015;37:511-517.
21. Wu M, Mohan C. B-cells in systemic sclerosis: emerging evidence from genetics to phenotypes. CurrOpinRheumatol 2015;27:537-541.
22. Murdaca G, Spanò F, Contatore M, Guastalla A, Puppo F. Potential use of TNF-α inhibitors in systemic sclerosis. Immunotherapy 2014;6:283-289.
23. Neeper M, Schmidt AM, Brett J, Yan SD, Wang F, Pan YC, *et al*. Cloning and expression of a cell surface receptor for advanced glycosylation end products of proteins. J BiolChem 1992;267:14998-15004.
24. Heizmann CW, Ackermann GE, Galichet A. Pathologies involving the S100 proteins and RAGE. SubcellBiochem 2007;45:93-138.
25. Leclerc E, Vetter SW. The role of S100 proteins and their receptor RAGE in pancreatic cancer. BiochimBiophysActa 2015;1852:2706-2711.
26. He M, Kubo H, Ishizawa K, Hegab AE, Yamamoto Y, Yamamoto H, *et al*. The role of the receptor for advanced glycation end-products in lung fibrosis. Am J Physiol Lung Cell MolPhysiol 2007;293:L1427-1436.
27. Queisser MA, Kouri FM, Königshoff M, Wygrecka M, Schubert U, Eickelberg O, *et al*. Loss of RAGE in pulmonary fibrosis: molecular relations to functional changes in pulmonary cell types. Am J Respir Cell MolBiol 2008;39:337-345.
28. Yan L, Mathew L, Chellan B, Gardner B, Earley J, Puri TS, *et al*. S100/Calgranulin-mediated inflammation accelerates left ventricular hypertrophy and aortic valvesclerosis in chronic kidney disease in a receptor for advanced glycation end products-dependent manner. ArteriosclerThrombVascBiol 2014;34:1399-1411.